



저작자표시-비영리-변경금지 2.0 대한민국

이용자는 아래의 조건을 따르는 경우에 한하여 자유롭게

- 이 저작물을 복제, 배포, 전송, 전시, 공연 및 방송할 수 있습니다.

다음과 같은 조건을 따라야 합니다:



저작자표시. 귀하는 원저작자를 표시하여야 합니다.



비영리. 귀하는 이 저작물을 영리 목적으로 이용할 수 없습니다.



변경금지. 귀하는 이 저작물을 개작, 변형 또는 가공할 수 없습니다.

- 귀하는, 이 저작물의 재이용이나 배포의 경우, 이 저작물에 적용된 이용허락조건을 명확하게 나타내어야 합니다.
- 저작권자로부터 별도의 허가를 받으면 이러한 조건들은 적용되지 않습니다.

저작권법에 따른 이용자의 권리는 위의 내용에 의하여 영향을 받지 않습니다.

이것은 [이용허락규약\(Legal Code\)](#)을 이해하기 쉽게 요약한 것입니다.

[Disclaimer](#)

공학석사 학위논문

**Aluminium phosphate-coated  
cathode material  
for high performance Li-ion battery**

AlPO<sub>4</sub> 코팅을 통한 LiNi<sub>0.8</sub>Co<sub>0.15</sub>Al<sub>0.05</sub>O<sub>2</sub>의  
리튬 이온전지 양극 소재로서의 성능향상

2019년 7월

서울대학교 대학원

공과대학 화학생물공학부

Song Kyungsun

## **Abstract**

# **Aluminium phosphate-coated cathode material for high performance Li-ion battery**

Song Kyungsun

School of Chemical & Biological Engineering

Seoul National University

As Lithium ion batteries(LIBs) are in demand for not only portable electric devices also various electrical vehicles, High energy density of LIBs are heavily required. This characteristic is mainly dependent to cathode materials used. Thus, plenty of research have been made to improve the degree of lithium utilization and specific energy density of cathode materials. Rate capability is also one of key issues for convenience and competitiveness of electrical vehicle, especially in case of BEV which is totally run by electrical power sources. Ni-rich layered lithium transition-metal oxides can be a brilliant solution at lower cost than the conventional  $\text{LiNi}_x\text{Co}_y\text{Mn}_{(1-x-y)}\text{O}_2$ . However, for these Ni-rich compounds there are still several bottlenecks regarding

their cycle life, reliability and safety caused by the side reaction between electrode and electrolyte.[2]

In this research, a simple interface engineering method, surface coating with aluminum phosphate by wet chemical method is introduced. The fact that coating layer is composed of two regions , Al-rich and P-rich, rather than single-phase  $\text{AlPO}_4$  is reported by Cho et al [1] and studied with X-ray photoelectron spectroscopy (XPS) in this research.

Compare to the pristine NCA,  $\text{AlPO}_4$ -coated NCA delivers high energy and retains cycle performance. Furthermore, it performs better in terms of rate capability in high voltage limit.(4.8V). These results suggest that  $\text{AlPO}_4$ -coated NCA material could act as one promising alternative for next-generation LIBs with high energy density and rate capability in the near future.

**Keywords:** Lithium ion batteries, Cathode, Nickel rich, Coating, Aluminum phosphate

**Student Number: 2017-24208**

# Contents

<b>Chapter 1. Introduction .....</b>	<b>6</b>
<b>Chapter 2. Experimental .....</b>	<b>10</b>
2.1 Preparation of material.....	10
2.2 Preparation of composite electrode .....	10
2.3 Preparation of half cell .....	11
2.4 Characterization .....	11
2.5 Electrochemical measurement.....	12
<b>Chapter 3 Results and discussion .....</b>	<b>13</b>
3.1 The analysis of powder .....	13
3.2 The electrochemical analysis .....	20
<b>Chapter 4 Conclusions .....</b>	<b>29</b>
<b>References .....</b>	<b>30</b>
<b>국문초록.....</b>	<b>32</b>

## List of Figures

<b>Figure 3.1</b>	X-ray diffraction patterns of the pure NCA material and AlPO <sub>4</sub> -coated NCA material .....	26
<b>Figure 3.2</b>	X-ray diffraction patterns of the pure NCA material and AlPO <sub>4</sub> -coated NCA material.....	27
<b>Figure 3.3</b>	SEM images and EDS mapping of the pristine(a) and AlPO <sub>4</sub> -coated NCA material (b).....	28
<b>Figure 3.4</b>	TEM images(cross-sectional) of the AlPO <sub>4</sub> -coated NCA material.....	30
<b>Fig. 3.5.a</b>	Voltage profiles of pristine/coated materials at 20 mA <sup>-1</sup> ..	21
<b>Fig. 3.5.b</b>	Voltage profiles of pristine/coated materials during cycletest at 200 mA g <sup>-1</sup> .....	21
<b>Fig. 3.6 (a)</b>	Cycle performance at 1.0 C-rate / 2.0C-rate .....	23
<b>Fig. 3.6 (b)</b>	Cycle performance at 5.0 C-rate / 10.0C-rate .....	24

**Fig. 3.7** Cycle voltammetry of Pristine and AlPO<sub>4</sub> at 0.5 mVsec<sup>-1</sup> and  
1.0mVsec<sup>-1</sup>for 10 cycles ..... 26

**Fig. 3.8.a** Rate capability of Pristine and AlPO<sub>4</sub> with 2.5V-4.5V  
range.....27

**Fig. 3.8.b** Rate capability of Pristine and AlPO<sub>4</sub> with 2.5V-4.2V  
range.....27

# Chapter 1. Introduction

As the pressure on natural resources and the environmental sustainability crisis grows, developing renewable energy and energy conservation are considered to be essential technical issues.[5] Consequently, energy storage technology is more crucial today than ever before. As the new type of portable energy storage device, lithium ion batteries (LIBs) are preferred to be used to various applications, including stationary energy storage, smart grid, electric vehicles.[6][7]

Increasing the energy density and saving the cost are main targets of developments in LIBs. The performance of LIBs are strongly dependent to the properties of the materials adapted.[8]

Layered structural  $\text{LiCoO}_2$  (LCO) has been widely used in small LIBs for mobile phones, cameras and laptops. However, its specific capacity is too small, with lithium utilization in the structure less than 60%, to be used for high energy devices.

Over the past decades, these requirements of higher utilization of lithium and specific energy density have been the main driving force for the advance of alternative layered structure compounds, such as olivine phosphates ( $\text{LiMPO}_4$ ; M = Fe, Co, Ni, and Mn) and spinel



oxides ( $\text{LiM}_2\text{O}_4$ ,  $M = \text{Mn, Ni}$  and  $\text{Co}$ ), however these have a low capacity.[9][10]

The layered structural compounds can be represented by the formula  $\text{LiMO}_2$  ( $M$  : transitional-metal elements), where the  $M$  and  $\text{Li}$  ions are located in octahedral sites in a face-centered cubic oxygen structure.  $\text{Li}$  slabs lie between  $\text{MO}_2$  slabs in the  $[111]$  direction of the cubic structure. Transitional-metal elements are typically electrochemically active materials including nickel, manganese or cobalt. It is widely established that the diffusion of  $\text{Li}^+$  ions in the layered structures occurs along a two-dimensional (2D) interstitial space, which is considered as a pathway for higher  $\text{Li}^+$  mobility. The  $\text{LiMO}_2$  cathode can produce a very large theoretical capacity of more than  $270 \text{ mAhg}^{-1}$  and a comparatively high working voltage above  $3.6 \text{ V}$  versus  $\text{Li}$  metal.[11]

Replacing  $\text{Co}$  and  $\text{Mn}$  with  $\text{Ni}$  in the layered structure results in higher utilization of lithium, increasing a capacity of  $220 \text{ mAhg}^{-1}$  with almost 80% reversible extraction of  $\text{Li}$  in the host structure.[12]

However, owing to the similar radius of  $\text{Li}^+$  ( $0.076 \text{ nm}$ ) and  $\text{Ni}^{2+}$  ( $0.069 \text{ nm}$ ), non-stoichiometric structures are usually found as the result of  $\text{Li}/\text{Ni}$  site-exchange. This phenomenon is termed cation mixing and causes various problems including capacity loss and

structure deterioration,[13] surface side reactions that accelerate capacity fade during cycling and high-temperature storage,[14] poor thermal stability, and dramatic heat release from the electrode if it becomes highly delithiated.[15]

Ni-based cathode materials have a strong tendency to take up moisture and they have a high concentration of residuals such as  $\text{Li}_2\text{CO}_3$  and  $\text{LiOH}$ . Other problems include severe gas evolution and deposition of insulating  $\text{LiF}$  from the decomposition of the surface impurities and electrolyte. [16].

To settle down these numerous drawbacks of Ni-based cathode materials, Changing the surface chemistry or providing physical protection layers. [17] In consideration of the importance of surface coating modification, a vast number of researches have been achieved on the modification of cathode materials by surface coating with a variety of coating materials and coating technologies.

Recently, the commonly used coating materials for cathode modifications are numerous oxides [18][19], active electrode materials [20][21], phosphate[22][23], carbon[24][25], and the coating technologies mainly include co-precipitation [26], sol-gel [27], vapor deposition [28], dry coating method [29]. These coatings can improve

the electrochemical performance of cathode material to some extent under certain conditions. Herein,  $\text{AlPO}_4$  is suggested and investigated as a coating material. A simple wet chemical coating of  $\text{AlPO}_4$  onto  $\text{LiNi}_{0.8}\text{Co}_{0.15}\text{Al}_{0.05}\text{O}_2$  improved energy density and rate capability in high voltage compared to the pristine material. Elucidation on the improvement are made using previous X-ray photoelectron spectroscopy (XPS) and transmission electron microscope (TEM) studies.[29]

## Chapter 2. Experimental

### 2.1 Preparation of material

AlPO<sub>4</sub>-coated LiNi<sub>x</sub>Co<sub>y</sub>Mn<sub>(1-x-y)</sub>O<sub>2</sub> (NCA) was prepared from NCA powder (L&F, < 20 micron) with wet chemical method [3]. Appropriate amounts of aluminum nitrate Al(NO<sub>3</sub>)<sub>3</sub>·9H<sub>2</sub>O and (NH<sub>4</sub>)<sub>2</sub>HPO<sub>4</sub> were dissolved in distilled water until a light white suspension solution (the AlPO<sub>4</sub> nanoparticle solution) was observed. NCA powders (with an average particle size of 10 μm) were then added to the coating solution slowly and mixed thoroughly. The slurry was then poured into a tray, dried in an oven for 6 h at 130 °C, and annealed at 700 °C for 5 h in a furnace.

### 2.2 Preparation of composite electrode

For the preparation of the working electrode, first of all, active material, super P (as a conductive agent) and polyvinylidene fluoride (as a binder) were stored in a convection oven at 100 °C for longer than 1 hour to eliminate moisture. Then a slurry composed of active material, super P and polyvinylidene fluoride (8:1:1 in weight ratio) in n-methyl-2-pyrrolidone was uniformly plastered on a Al foil and dried in a

vacuum oven at 120 °C for 10 hour. After drying, the electrode was roll-pressed and Eleven millimeter diameter electrode disks were punched and redried under a vacuum at 120 °C for 30 min before being kept in an argon-filled glovebox.

### **2.3 Preparation of half cell**

2032 type coin cell were assembled with a Al foil electrode (20  $\mu\text{m}$  thick, 11 mm in diameter), a polypropylene separator, lithium metal foil as a counter electrode and a reference electrode, and the electrolyte was 1.0 M  $\text{LiPF}_6$  dissolved in ethylene carbonate (EC) and diethyl carbonate (DEC) (1:1 in volume ratio). All processes were performed in an argon-filled glove box. Assembled coin cells were allowed to soak overnight and then began electrochemical testing on a 'WBCS3000 cyclor (WonA Tech, Korea) at room temperature.

### **2.4 Characterization**

X-Ray diffraction (XRD) patterns were obtained on a Bruker D-5005 with  $\text{Cu K}\alpha$  radiation ( $\lambda = 1.5406 \text{ \AA}$ ) at 40 kV and 40 mA with a scan range of  $10^\circ\sim 90^\circ$ . X-ray photoelectron spectroscopy (XPS) experiments were performed by AXIS-His spectrometer (KRATOS) with a monochromatic  $\text{Al K}\alpha$  source (1486.6 eV) with at 12 kV and 10

mA current. The binding energies were shifted for charging using C1s to 284.6 eV. The morphologies of samples were characterized by conducting field emission scanning electron microscopy (FE-SEM, Carl Zeiss AURIGA). In addition, A JEM-F200 transmission electron microscope (TEM) equipped with a field emission gun and operated at 200 kV was used to examine the cross-sectional microstructure of the coating layer. the sample was prepared by embedding the AlPO<sub>4</sub>-coated NCA powder in a clear epoxy resin and then microtoming slices of 30 nm thickness.for high-resolution TEM measurements.

## **2.5 Electrochemical measurement**

The principal voltage window was between 2.5V and 4.5 V vs. Li/Li<sup>+</sup>. The cells were galvanostatically charged and discharged at room temperature. The loading level is about 3 mg cm<sup>-2</sup>. In term of capacity of the cathode active material, it is based on the total weight of composite. Rate capability tests were made with a few c-rates which are from 0.5 C-rate to 10.0 C-rate. (0.5C/1.0C/2.0C/5.0C/10.0C). Cyclic voltammetry (CV) was also conducted with three different scan rates (0.1mVs<sup>-1</sup>. / 0.5mVs<sup>-1</sup>/1.0mVs<sup>-1</sup>). All electrochemical tests were carried out with a WBCS3000 cyler (WonA Tech, Korea)

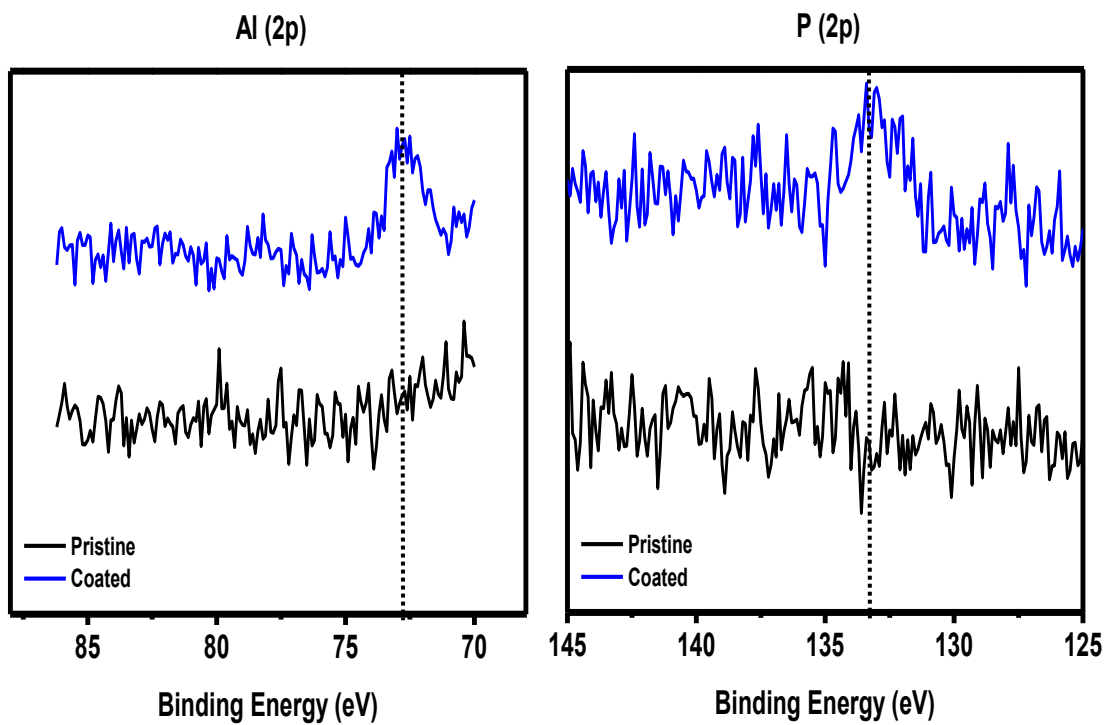
## Chapter 3. Results and discussion

### 3.1 The analysis of powder

The analysis by XPS confirmed the existence of strong P=O bond (Figure 3-1). It should be noted that a peak at 133.4 eV can be seen in the P 2p spectra of the coated NCA, which can be attributed to the strong P=O bond according to the previous reports [30][31][32].

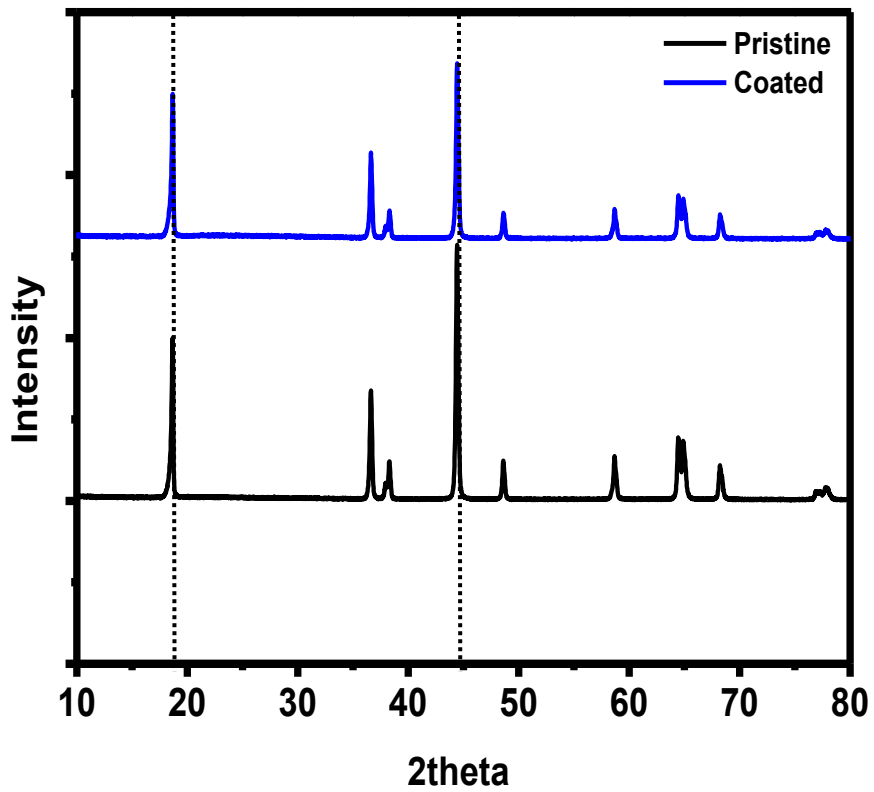
So we believed that the presentation of the coating layer on the surface of NCA could avoid the direct exposure of NCA to electrolyte, thus effectively suppresses the side reactions between them.

Figure 3-2 shows the X-ray diffraction patterns of the pure NCA material and AlPO<sub>4</sub>-coated NCA material. After coating and high temperature calcination, a small amount of Al<sup>3+</sup> may be doped into the Li<sup>+</sup> site caused by crystal expansion. This result clarifies that the surface modified NCA material possesses layered  $\alpha$ -NaFeO<sub>2</sub> structure (R-3m space group). And no impurity phase is observed in the XRD patterns of the modified samples [33][34][35] indicating that the structure of the surface coated material did not change obviously compared with the bare material.



**Fig. 3.1** X-ray diffraction patterns of the pure NCA material and AlPO<sub>4</sub>-coated NCA material





**Fig. 3.2** X-ray diffraction patterns of the pure NCA material and AlPO<sub>4</sub>-coated NCA material

SEM secondary electron images of bare NCA and AlPO<sub>4</sub>-coated NCA particles are compared in images of in Figure 3.3(a)

The rounded morphology of bare particles is in good agreement with the hypothesis that bare NCA is lithium overstoichiometric, as stoichiometric NCA produced at high temperatures such as 1000 °C are typically in plate-like shape. The surface of the bare NCA particle appears to be fairly smooth, whereas most of the surface of AlPO<sub>4</sub>-coated NCA particles is rough. Additionally EDS mapping was conducted to understand the distribution of elements of Aluminum and Phosphorus indicating the homogeneity of coating layer. Observing the figure 3.3(b), we are able to find inhomogeneity of coating layer and it is in accordance with the XPS previous data (figure 3.1). it suggests that reactions between AlPO<sub>4</sub> nanoparticles and bare NCA during the heat-treatment step lead to formation of Al-rich regions, namely, Li<sub>1-y</sub>Al<sub>y</sub>O<sub>2</sub> with high Al content, and P-rich regions, namely, Li<sub>3</sub>PO<sub>4</sub>, on the particle surface.

To gain further insight on the microstructure of AlPO<sub>4</sub>-coated NCA, we performed TEM studies of microtomed AlPO<sub>4</sub>-coated NCA particles Typical cross-sectional TEM images of an “AlPO<sub>4</sub>”-coated NCA particle or crystal are shown in Figure 3.4, where reveals the microstructure of the outer edge of the particle. The coating layer

appeared to cover most of the particle surface but it was found that the thickness was not uniform on the micrometer-scale with a thickness variation of 10-100 nm. This observation is also consistent with the pitted surface found in the SEM images (Figure 3.3).

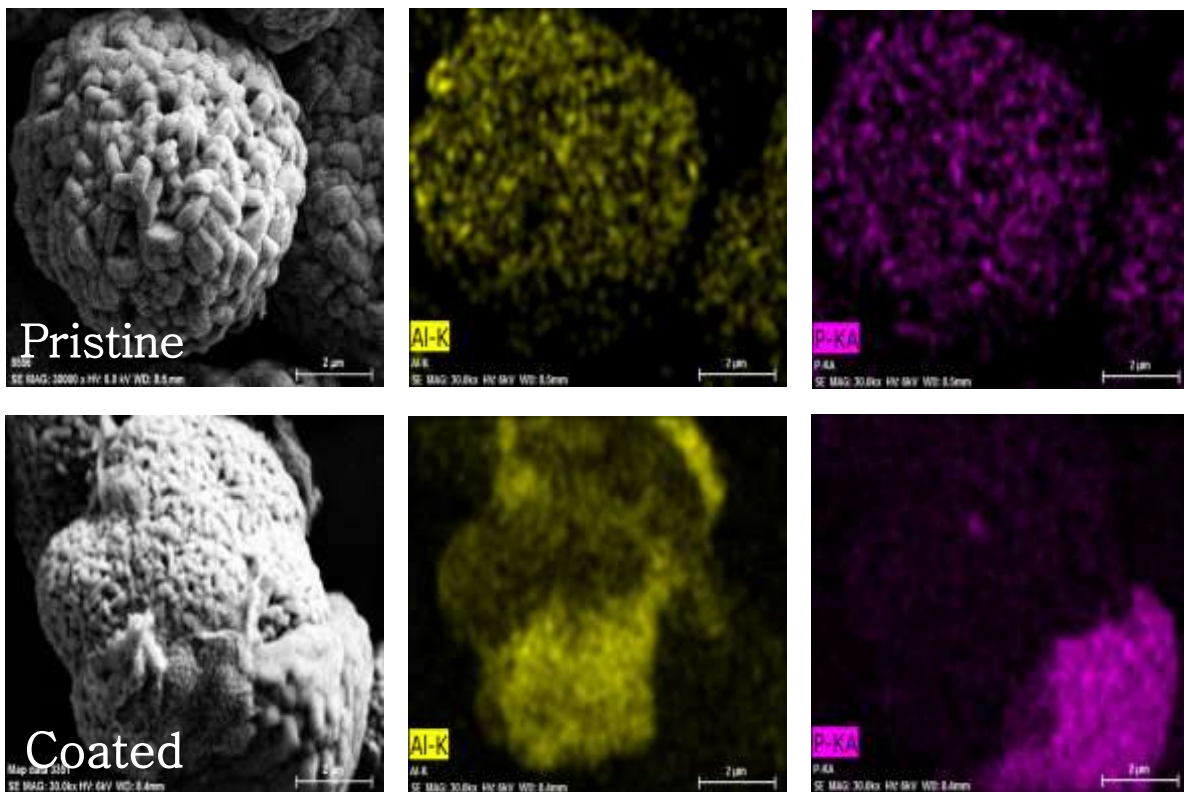


**Fig. 3.3** SEM images and EDS mapping of the pristine(a) and AlPO<sub>4</sub>-coated material(b)

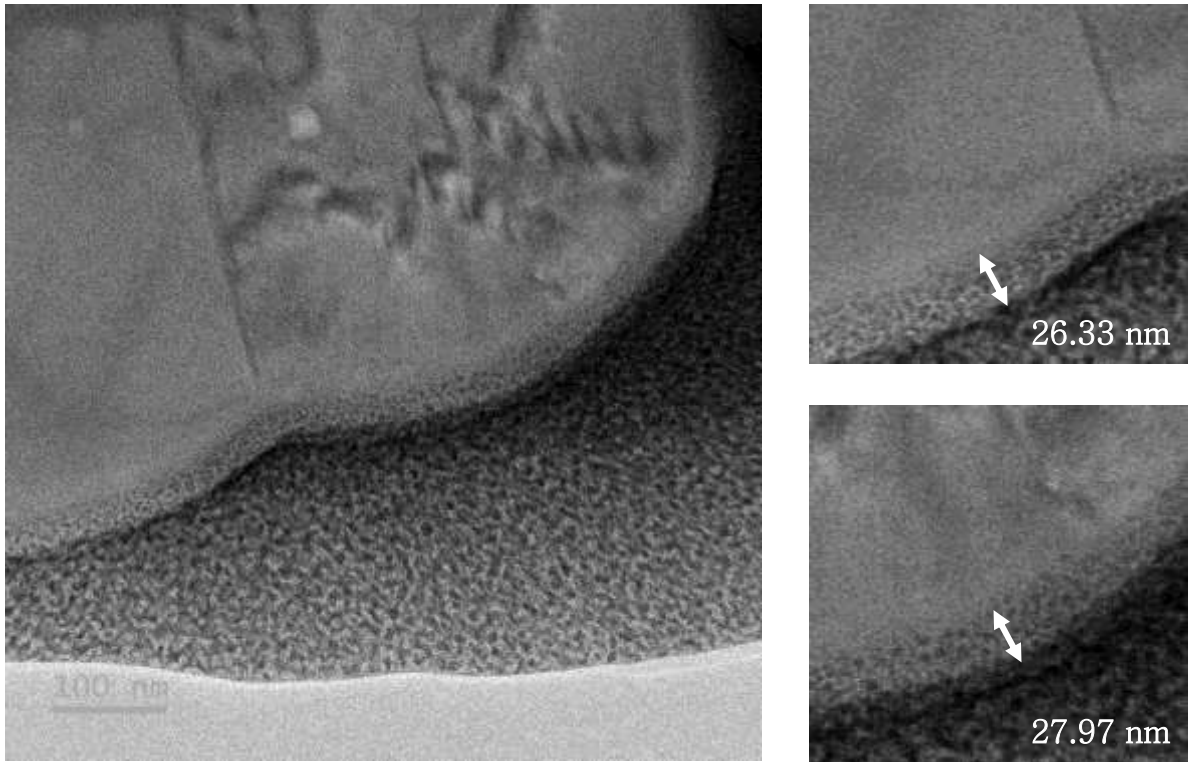
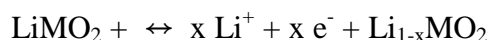


**Fig. 3.4** (a) XRD patterns of GO, NG and M-NG composite, (b) TGA curve of M-NG composite.

### 3.2 The electrochemical analysis

To evaluate the performance of lithium batteries with  $\text{AlPO}_4$  electrode, the cells were galvanostatically charged and discharged between 4.5 V and 2.5 V. In this voltage range, the mechanism underlying the reaction between lithium and cathode material (NCA) can be described by the following electrochemical conversion:[36]



At a current density of  $20 \text{ mA g}^{-1}$  (Fig. 3.5.a), the first discharge capacity of M-NG was  $201 \text{ mA h g}^{-1}$ . In the first discharge curve, the voltage profile of  $\text{AlPO}_4$  -coated material presents higher energy density compared to the pristine material. there are a gap between the amount of overpotential of two curves. In Fig.3.5.b, it is able to find that cycle stability of  $\text{AlPO}_4$  -coated material presents an advantage relatively.

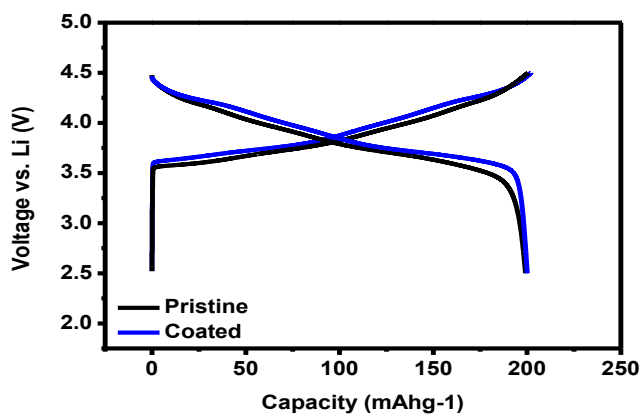


**Fig. 3.5.a** Voltage profiles of pristine/coated materials at  $20 \text{ mA g}^{-1}$

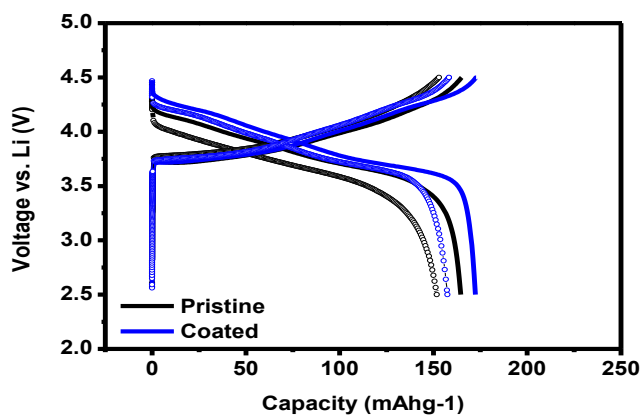


**Fig. 3.5.b** Voltage profiles of pristine/coated materials during cycle test at  $200 \text{ mA g}^{-1}$  (cycle number: 30)

In figure 3.6.a, At a C-rate of 1C/2C, it obviously presents the effect of coating layer in terms of cycle stability. the amount of overpotential around 3.6V (vs.Li/Li<sup>+</sup>) and 4.2V(vs.Li/Li<sup>+</sup>) decreased in case of AlPO<sub>4</sub> coated material. whereas, in figure 3.6.b, At a C-rate of 5C/10C, it probably seems that the effect of coating layer decreased in first cycle. However, the degradation during cycle test of AlPO<sub>4</sub> presents less compared to pristine material.



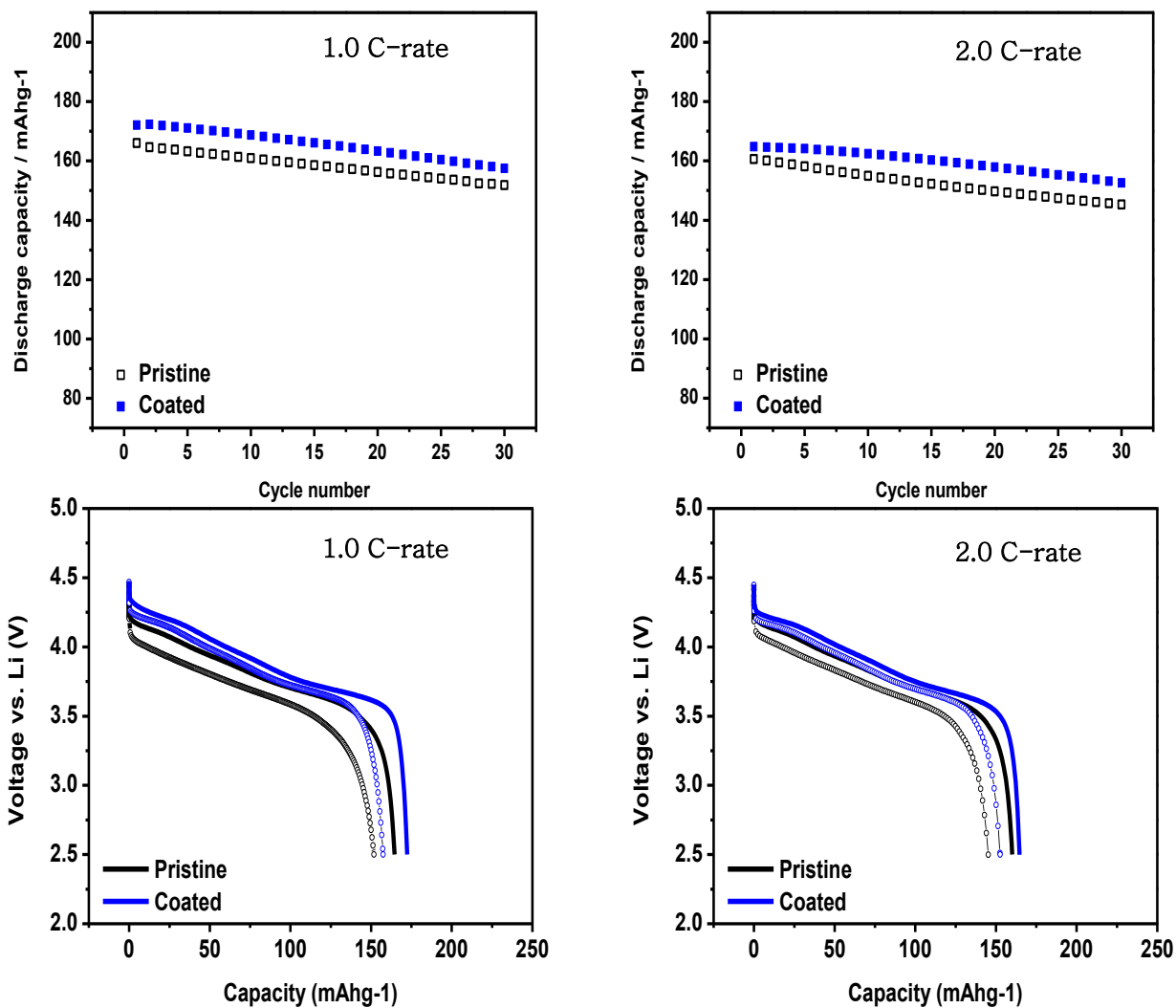


**Fig. 3.6** (a) Cycle performance at 1.0 C-rate / 2.0C-rate (30 cycle)

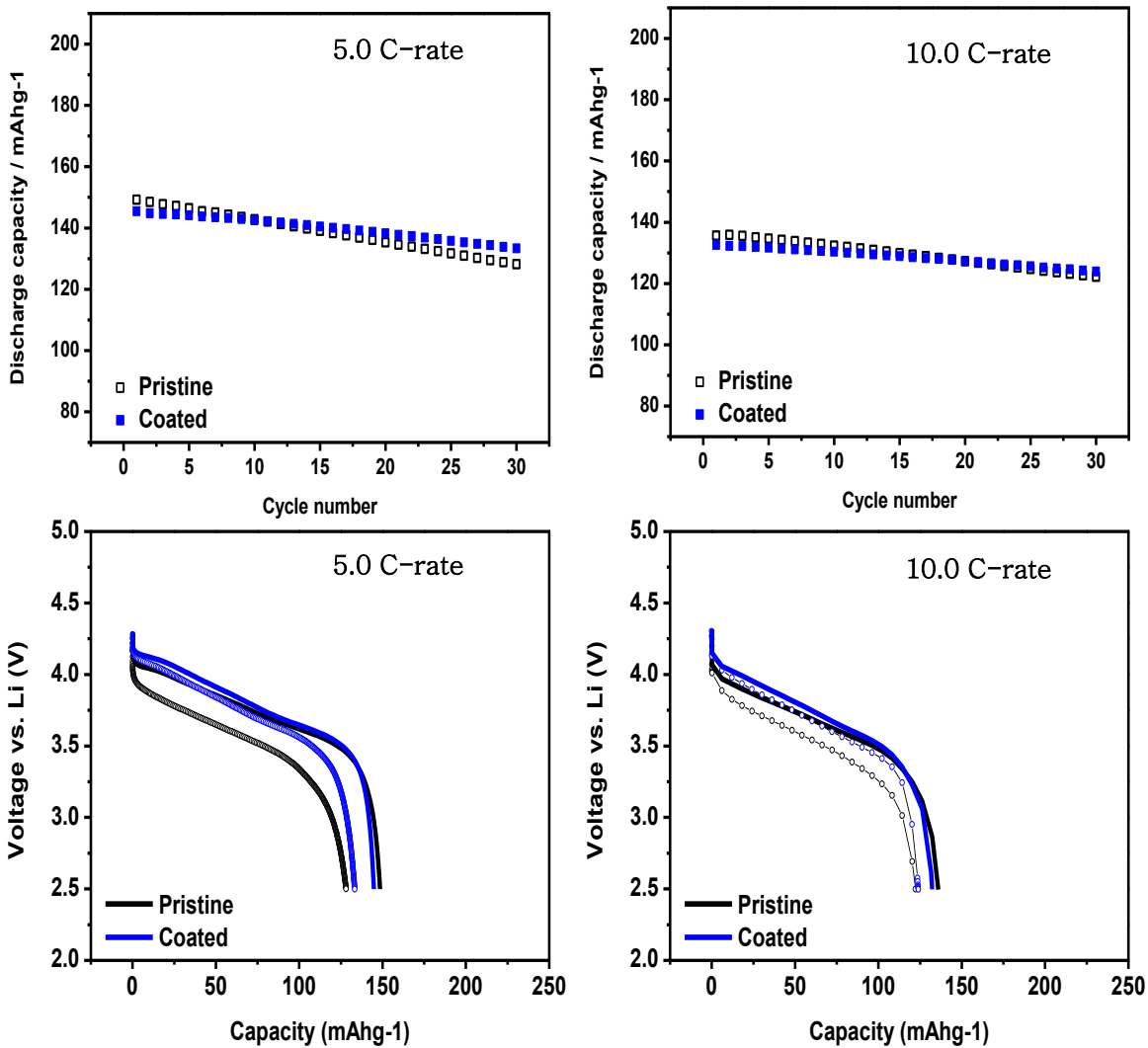


**Fig. 3.6 (b)** Cycle performance at 5.0 C-rate / 10.0C-rate (30 cycle)

In figure 3.7, the voltammetry of both material present similar phenomenon. they show two couples of redox peaks. First redox peaks around 3.6V come from the oxidation of Ni from Ni<sup>3+</sup> to Ni<sup>4+</sup>, involving the phase transitions from hexagonal to monoclinic (H1 to M) and monoclinic to hexagonal (M to H2), respectively, and contributing to the main capacity of NCA[37]. Second redox peaks around 4.35V from the oxidation of Co from Co<sup>3+</sup> to Co<sup>4+</sup>, involving the phase transitions from hexagonal to hexagonal (H2 to H3) and contributing to the additional capacity of NCA.

Based on the elucidation above, it is noted that there is a difference in a first cycle with 1.0 mVsec<sup>-1</sup>. It is clear that the first peak of pristine NCA presents the lack of oxidation of transitional metals, Ni/Co, on the other hand the first peak of AlPO<sub>4</sub>-coated NCA presents the original behavior, and we are able to it is the reason for the high-rate capability of AlPO<sub>4</sub>-coated NCA.

In Figure 3.8, we are able to verify the gap of rate capability between two samples. Especially with 4.5V upper voltage limit, it presents that there are more gap between the pristine and AlPO<sub>4</sub> and it suggests that the advantage of AlPO<sub>4</sub>-coated NCA is maximized with high voltage over 4.35V.

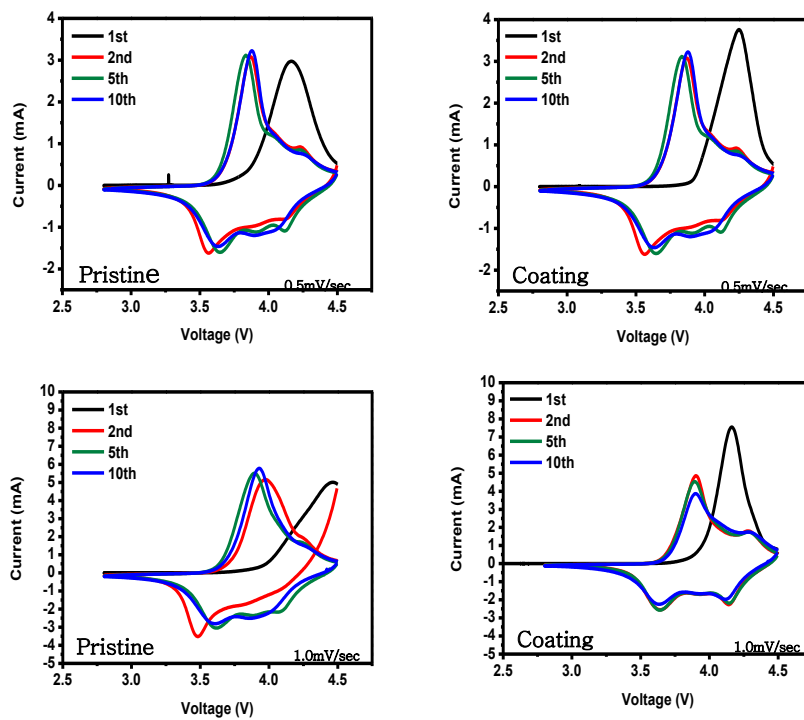


**Fig. 3.7** Cycle voltammetry of Pristine and AlPO<sub>4</sub> at 0.5 mVsec<sup>-1</sup> and 1.0 mVsec<sup>-1</sup> for 10 cycles.

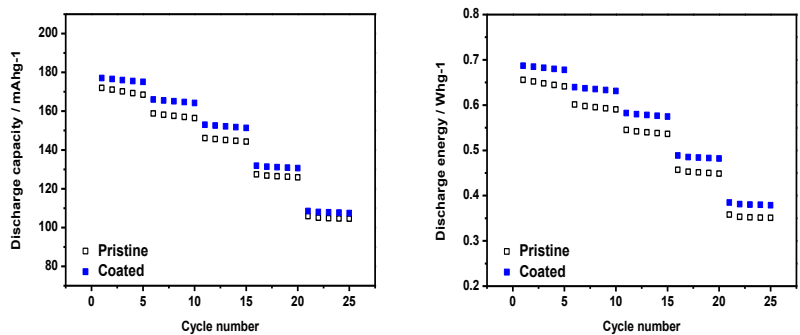


**Fig. 3.8.a** Rate capability of Pristine and AlPO<sub>4</sub> with 2.5V-4.5V range

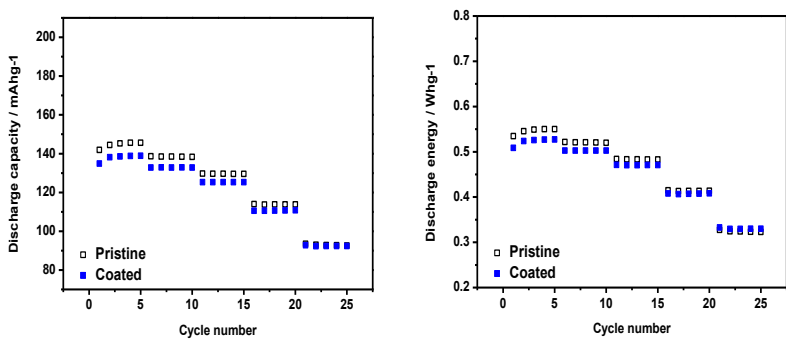


**Fig. 3.8.b** Rate capability of Pristine and AlPO<sub>4</sub> with 2.5V-4.2V range

## Chapter 5. Conclusions

In summary, We have successfully improved the electrochemical performances of NCA by effective  $\text{AlPO}_4$  coating by the simple wet chemical procedure. With the process of coating, the improved Energy density is obtained for the surface modified NCA.

The modified sample shows much better rate capability and cycle stability, especially in high voltage over 4.35V. The results indicate that the coating materials derived from  $\text{AlPO}_4$  can act as a stable layer to protect the active material and suppress side reactions between NCA and the electrolyte. Therefore,  $\text{AlPO}_4$  coating layer to modify the sample surface is a viable method to improve the energy density and rate capability of NCA in high voltage. This research will open new options to improve the properties of other related electrode materials for rechargeable batteries in the near future.

## References

- [1] Chem. Mater. 2007, 19, 5748-5757
- [2] J Mater Chem A, 2013,1: 4879–4884
- [3] Electrochemistry Communications 5 (2003) 146–148
- [4] Journal of The Electrochemical Society, 151 ~10! A1707-A1711 ~2004
- [5] Adv. Funct. Mater. 2013, 23, 929 – 946
- [6] Dunn, H. Kamath, J. M.Tarascon, Science 2011, 334, 928 – 935
- [7] Energy Environ. Sci. 2012, 5, 7854 – 7863.
- [8] Acc. Chem. Res. 2013, 46, 1226 –1238
- [9] Mater. Sci. Eng. R 2012, 73, 51 – 65
- [10] J. Mater. Chem. 2012, 22, 3680 – 3695
- [11] J. Solid State Electrochem. 2009, 13, 1157 – 1164
- [12] Science 2011, 334, 928 – 935
- [13] Energy Environ. Sci. 2014, 7, 1068 – 1078.
- [14] J. Power Sources 2003, 119 – 121, 497 – 503
- [15] J. Electrochem. Soc. 2011, 158, R1 – R25
- [16] Angew. Chem. Int. Ed. 2015, 54, 4440 – 4457
- [17] Journal of Alloys and Compounds 706 (2017) 24-40
- [18] Adv. Energy Mater. 3 (2013) 213-219.
- [19] Chem. Mater. 26 (2014) 2537-2543.
- [20] Electrochim. Acta 147 (2014) 626-635
- [21] Chem. Eur. J. 20 (2014) 824-830.
- [22] Powder Technol. 287 (2016) 77-81.
- [23] ACS Appl. Mater. Interfaces 8 (2016) 15225-15231
- [24] J. Mater. Chem. A3 (2015) 996-1004
- [25] J. Solid State Electrochem. 19 (2015) 1523-1533
- [26] Appl. Phys. Lett. 105 (2014), 143904-143904-3
- [27] J. Power Sources 314 (2016) 85-92
- [28] J. Electrochem. Soc. 157 (2010) A625-A629

- [29] Chem. Mater. 2007, 19, 5748-5757
- [30] Chem Commun, 2015, 51: 2943–2945
- [31] Nature, 2010, 464: 392–395
- [32] Chem Mater, 2007,19: 5748–5757
- [33] J Mater Chem A, 2016, 4: 8350–8358
- [34] Mater Res Bull, 2012, 47:2830–2833
- [35] Chem Mater, 2015, 27:526–536
- [36] Nature Matt. 11.19
- [37] ACS Appl. Mater. Interfaces, 2016, 8, 1297–1308.



## 초 록

리튬 이온 배터리 (LIB)는 휴대용 전기 장치뿐만 아니라 에너지 저장장치(ESS), 전기 자동차(Electrical Vehicle)에 대한 수요로 인하여 높은 에너지 밀도가 요구되고 있다.

배터리의 특성은 주로 사용되는 양극 소재에 따라 달라지고, 해당 물질의 리튬 이용률 및 비 에너지 밀도를 향상시키기 위한 많은 연구가 이루어졌다. 더불어, 가격 경쟁력은 전기 자동차의 경쟁력과 일반 운전자의 구매력에 지대한 영향을 미치는데, 이는 순수 전기차인 BEV의 경우 더 지대하다.

Ni-rich한 NCA는 층상 전이 금속 산화물은 기존의

$\text{LiNi}_x\text{Co}_y\text{Mn}_{(1-x-y)}\text{O}_2$ 보다 저렴한 비용으로 뛰어난 솔루션이 될 수 있다. 다만 Ni-rich 산화물의 경우 전극과 전해액 사이의 부반응으로 인한 사이클 수명, 신뢰성 및 안전성과 관련하여 개선되어야 할 점이 여전히 존재한다.

본 연구에서는 간단한 wet chemical coating에 의한  $\text{AlPO}_4$ 을 이용한 표면 코팅기술을 소개한다.  $\text{AlPO}_4$  단일상이 아닌 Al-rich와 P-rich의 2 개의 상으로 존재함이 이미 보고 되었기 때문에, 이를 XPS로 관찰하고, 고전압대에서의 전기화학적 이점을 확인하고자 한다.

주요어 : 리튬이온전지, 양극, Ni-rich, 코팅,  $\text{AlPO}_4$

학 번 : 2017-24208